J|A|C|S ARTICLES

Published on Web 10/20/2009

Zeolitic Polyoxometalate-Based Metal−Organic Frameworks (Z-POMOFs): Computational Evaluation of Hypothetical Polymorphs and the Successful Targeted Synthesis of the Redox-Active Z-POMOF1

L. Marleny Rodriguez-Albelo,[†] A. Rabdel Ruiz-Salvador,*[,†] Alvaro Sampieri,[‡] Dewi W. Lewis,[‡] Ariel Gómez,[§] Brigitte Nohra,[⊥] Pierre Mialane,[⊥] Jérôme Marrot,[⊥] Francis Sécheresse,[⊥] Caroline Mellot-Draznieks,*[,‡] Rosa Ngo Biboum,[∥] Bineta Keita,*[,∥] Louis Nadjo,[∥] and Anne Dolbecq*[,⊥]

Zeolite Engineering Laboratory, Institute of Materials Research and Engineering (IMRE), University of Havana, Havana 10400, Cuba, Department of Chemistry, University College London, 20 Gordon Street, London, WC1H 0AJ, U.K., Department of Physics, University of Guelph, Ontario N1G 2W1 Canada, Institut Lavoisier de Versailles, UMR 8180, Université de Versailles Saint-Quentin en Yvelines, 45 Avenue des Etats-Unis, 78035 Versailles cedex, France, and Laboratoire de Chimie Physique, Groupe d'Electrochimie et de Photoélectrochimie, UMR 8000, CNRS, Université Paris-Sud, Bâtiment 350, 91405 Orsay cedex, France

Received June 25, 2009; E-mail: rabdel@imre.oc.uh.cu; c.mellot-draznieks@ucl.ac.uk; bineta.keita@lcp.u-psud.fr; dolbecq@chimie.uvsq.fr

Abstract: The targeted design and simulation of a new family of zeolitic metal−organic frameworks (MOFs) based on benzenedicarboxylate (BDC) as the ligand and ε-type Keggin polyoxometalates (POMs) as building units, named here Z-POMOFs, have been performed. A key feature is the use of the analogy between the connectivity of silicon in dense minerals and zeolites with that of the ε-type Keggin POMs capped with Zn(II) ions. Handling the ε-Keggin as a building block, a selection of 21 zeotype structures, together with a series of dense minerals were constructed and their relative stabilities computed. Among these Z-POMOFs, the cristobalite-like structure was predicted to be the most stable structure. This prediction has been experimentally validated by the targeted synthesis of the first experimental Z-POMOF structure, which was strikingly found to possess the cristobalite topology, with three interpenetrated networks. Crystals of $[NBu_4]_3[PMo^{V}_8Mo^{VI}_4O_{36}(OH)_4Zn_4(BDC)_2]\cdot 2H_2O$ (Z-POMOF1) have been isolated under hydrothermal conditions from the reduction of ammonium heptamolybdate in the presence of phosphorous acid and Zn(II) ions. Tetrabutylammonium cations play the role of counterions and space-filling agents in this tridimensional interpenetrated framework. Moreover, the electrochemistry of the ε-Keggin POM is maintained and can be exploited in the insoluble Z-POMOF1 framework, as demonstrated by the electrocatalytic reduction of bromate.

Introduction

Hybrid organic−inorganic materials have attracted considerable interest in the recent past due to their spectacular crystal structures and properties.[1,2] They display an extremely large number of topologies, from molecular complexes and layered coordination polymers to three-dimensional metal−organic frameworks (MOFs).[3] These solids have major potential impact in adsorption and separation processes.[4] Additionally, these materials can exhibit interesting magnetic, optical, and electronic properties,[5] although only a few reports exist of their electrochemical behavior.[6] Polyoxometalates (POMs) are primarily soluble anionic metal oxide clusters with a wide range of magnetic, redox, and catalytic properties.[7] In addition, they have also been regarded as building units for the design of POM-based MOFs, so-called POMOFs.[8,9] The combination of the

[†] University of Havana.
[‡] University College London.
[§] University of Guelph.
[⊥] Université de Versailles Saint-Quentin en Yvelines.
[∥] Université Paris-Sud.

(1) (a) Férey, G.; Mellot-Draznieks, C.; Serre, C.; Millange, F. *Acc. Chem. Res.* **2005**, *38*, 217. (b) Rosseinsky, M. J. *Microporous Mesoporous Mater.* **2004**, *73*, 15. (c) Maspoch, D.; Ruiz-Molina, D.; Veciana, J. *Chem. Soc. Rev.* **2007**, *36*, 770.
(2) (a) Rowsell, J. L. C.; Yaghi, O. M. *Microporous Mesoporous Mater.* **2004**, *73*, 3. (b) James, S. L. *Chem. Soc. Rev.* **2003**, *32*, 276. (c) Yaghi, O. M.; O'Keefe, M.; Ockwig, N. W.; Chae, H. K.; Eddaoudi, M.; Kim, J. *Nature* **2003**, *423*, 705.
(3) Cheetham, A. K.; Rao, C. N. R.; Feller, R. K. *Chem. Commun.* **2006**, 4780.
(4) (a) Kitagawa, S.; Uemura, K. *Chem. Soc. Rev.* **2005**, *34*, 109. (b) Latroche, M.; Surble, S.; Serre, C.; Mellot-Draznieks, C.; Llewellyn, P. L.; Lee, J.-H.; Chang, J.-S.; Jhung, S. H.; Férey, G. *Angew. Chem., Int. Ed.* **2006**, *45*, 8227. (c) Eddaoudi, M.; Kim, J.; Rosi, N.; Vodak, D.; Wachter, J.; O'Keeffe, M.; Yaghi, O. M. *Science* **2002**, *295*, 469. (d) Banerjee, R.; Phan, A.; Wang, B.; Knobler, C.; Furukawa, H.; O'Keeffe, M.; Yaghi, O. M. *Science* **2008**, *319*, 939.
(5) (a) Rao, C. N. R.; Cheetham, A. K.; Thirumurugan, A. *J. Phys.: Condens. Matter* **2008**, *20*, 1. (b) Kepert, C. J. *Chem. Commun.* **2006**, 695.

 10.1021/ja905009e CCC: $40.75

properties of POMs, with their diverse coordination modes, together with a knowledge of their ability to form POMOFs with a large variety of organic linkers, provides an impetus for the synthesis of these potentially multifunctional materials. Furthermore, the extensive electrochemical activity of POMs may be further exploited if they can be retained in an insoluble framework, opening avenues in fields such as sensors.

In extended POM materials, the inter-POM connectivity is generally achieved through grafted transition metal complexes, although we also note a very few exceptions, such as the coordination network of hexavanadate POMs functionalized by benzoate-terminated ligands linked by Tb(III) ions.[10] In this context, it is worth noting that only a few attempts have been reported of POMs linked by rigid carboxylates[9,11,12] (a particularly common linking motif in the MOF area). While a growing number of chain (1-D)[13] and layered (2-D)[14] POMOFs have been hydrothermally synthesized, only a limited number of 3-D POMOF frameworks have been described. Focusing on materials with POM−M−L−M−POM linkages (where M = 3d, 4d, or 4f metal, L = organic ligand), 3-D POMOFs include a network of $\{Ni_6PW_9O_{37}\}$ units connected by 1,2,4-BTC (BTC = benzenetricarboxylate) ligands,[9] molybdophosphonates linked through copper complexes,[15] and a chiral net of Keggin ions linked by copper−amino acid complexes.[16] Some of us have also developed a strategy for the synthesis of POMOFs at room temperature by using the ε-$\{PMo_{12}O_{40}\}$ Keggin ion capped by four La(III) ions (denoted ε-La), which with 1,3,5-BTC linkers results in a 3-D POMOF.[11]

The general philosophy for designing new extended solids has been the replacement of small building blocks with larger ones, using the reticular chemistry concepts.[17] We expect to be able to identify key features of a particular topology which may lend itself to synthesis as, for example, a POMOF. Moreover, computational evaluation of the stability of hypothesized frameworks can guide our search for viable synthesis targets, as previously described for zeotypes and related materials.[18] In the area of POMOFs, there has, to our knowledge, been only one attempt, from our group, to simulate such structures,[11] but to date, no relationship has been established between structure and stability. Still, the possibility of designing 3-D POMOFs is attractive because topochemically selected reactions govern the construction process of the hybrid framework under hydrothermal conditions. Under such conditions—as the POM building blocks are deemed to retain their integrity—an appropriate choice of organic ligands and reaction conditions may lead to a preidentified 3-D crystal structure. This concept is illustrated by numerous successful examples of transition metal-based MOFs in the literature[19] but is yet to be proven in the field of POMOFs.

In this program of work, our stated aim was to explore and synthesize a new family of MOFs, specifically 3-D POMOFs possessing tetrahedral nets, typified by dense silica polymorphs and zeotypes. We refer to these structures as Z-POMOFs. Over 180 unique zeotype topologies are known experimentally,[20] and a number of MOFs have also been synthesized with zeolite topologies,[21] either fortuitously or rationally, as illustrated by the recent discovery of the zeolitic imidazole frameworks (ZIFs).[22] Many more are likely. We postulate, therefore, that Z-POMOFs may be synthesized possessing extended zeolite-like networks.

We report here our strategy, whereby we devised methods to first construct and then evaluate the stability of a number of hypothetical Z-POMOFs. We then set about a targeted synthesis of the more viable structures and are able to report the first tetrahedrally connected network comprising a POM linked through organic ligands, denoted Z-POMOF1, possessing an interpenetrated cristobalite-like (or diamond) topology, which was predicted to be the most stable candidate by our modeling. We also show, for the first time, the electrocatalytic behavior of POMOFs, specifically that Z-POMOF1 exhibits high activity for the reduction of bromate.

Methods

Design Strategy. We describe first our strategy for selecting the systems to explore and our reasoning for the selection of the POM and organic linker. Having zeotypes in mind, the key requirements

(6) (a) Férey, G.; Millange, F.; Morcrette, M.; Serre, C.; Doublet, M.-L.; Grenèche, J.-M.; Tarascon, J.-M. *Angew. Chem., Int. Ed.* **2007**, *46*, 3259. (b) Doménech, A.; García, H.; Doménech-Carbó, M.-T.; Llabrés-i-Xamena, F. *J. Phys. Chem. C* **2007**, *111*, 13701. (c) Wang, X.-L.; Lin, H.-Y.; Liu, G.-C.; Zhao, H.-Y; Chen, B.-K. *J. Organomet. Chem.* **2008**, *693*, 2767.

(7) (a) Clemente-Juan, J. M.; Coronado, E. *Coord. Chem. Rev.* **1999**, *193−195*, 361. (b) Special issue on polyoxometalates: *J. Mol. Catal. A* **2007**, *1−2*, 1−242. (c) Mialane, P.; Dolbecq, A.; Sécheresse, F. *Chem. Commun.* **2006**, 3477.

(8) Streb, C.; Ritchie, C.; Long, D.-L.; Kögerler, P.; Cronin, L. *Angew. Chem., Int. Ed.* **2007**, *46*, 7579.

(9) Zheng, S.-T.; Zhang, J.; Yang, G.-Y. *Angew. Chem., Int. Ed.* **2008**, *47*, 3909.

(10) Han, J. W.; Hill, C. L. *J. Am. Chem. Soc.* **2007**, *129*, 15094.

(11) Dolbecq, A.; Mellot-Draznieks, C.; Mialane, P.; Marrot, J.; Férey, G.; Sécheresse, F. *Eur. J. Inorg. Chem.* **2005**, 3009.

(12) Dolbecq, A.; Mialane, P.; Lisnard, L.; Marrot, J.; Sécheresse, F. *Chem.−Eur. J.* **2003**, *9*, 2914.

(13) (a) Tian, A.; Ying, J.; Peng, J.; Sha, J.; Zhu, D.; Pang, H.; Zhang, P.; Chen, Y.; Zhu, M. *Inorg. Chem. Commun.* **2008**, *11*, 1133. (b) Tian, A.; Han, Z.; Peng, J.; Sha, J.; Zhao, Y.; Pang, H.; Zhang, P.; Zhu, M. *Solid State Sci.* **2008**, *10*, 1352.

(14) (a) Yi, Z.-H.; Cui, X.-B.; Zhang, X.; Xu, J.-Q.; Yang, G.-D.; Chen, Y.; Wang, T.-G.; Yu, X.-Y. *J. Mol. Struct.* **2008**, 149. (b) Zhang, Z.; Liu, J.; Wang, E.; Qin, C.; Li, Y.; Qi, Y.; Wang, X. *Dalton Trans.* **2008**, 463.

(15) Burkholder, E.; Golub, V.; O'Connor, C. J.; Zubieta, J. *Inorg. Chem.* **2003**, *42*, 6729.

(16) (a) An, H.-Y.; Wang, E.-B.; Xiao, D.-R.; Li, Y.-G.; Su, Z.-M.; Xu, L. *Angew. Chem., Int. Ed.* **2006**, *45*, 904. (b) An, H.; Xu, T.; Wang, E; Meng, C. *Inorg. Chem. Commun.* **2007**, *10*, 1453. (c) An, H.; Li, Y.; Xiao, D.; Wang, E.; Sun, C. *Cryst. Growth Des.* **2006**, *6*, 1107.

(17) (a) Yaghi, O. M.; O'Keeffe, M.; Ockwig, N. H.; Chae, H. K.; Eddaoudi, M.; Kim, J. *Nature* **2003**, *423*, 705. (b) Eddaoudi, M.; Kim, J.; Rosi, N.; Vodak, D.; Wachter, J.; O'Keeffe, M.; Yaghi, O. M. *Science* **2002**, *295*, 469. (c) Eddaoudi, M.; Moler, D. B.; Li, H. L.; Chen, B. L.; Reineke, T. M.; O'Keeffe, M.; Yaghi, O. M. *Acc. Chem. Res.* **2001**, *34*, 319.

(18) (a) Friedrichs, O. D.; Dress, A. W. M.; Huson, D. H.; Klinowski, J.; Mackay, A. L. *Nature* **1999**, *400*, 644. (b) Mellot-Draznieks, C.; Girard, S.; Férey, G. *J. Am. Chem. Soc.* **2002**, *124*, 15326. (c) Foster, M. D.; Simperler, A; Bell, R. G.; Friedrichs, O. D.; Paz, F. A. A.; Klinowski, J. *Nat. Mater.* **2004**, *3*, 234. (d) Woodley, S. M.; Catlow, C. R. A. *Nat. Mater.* **2008**, *7*, 937.

(19) Ockwig, N. W.; Delgado-Friedrichs, O.; O'Keeffe, M.; Yaghi, O. M. *Acc. Chem. Res.* **2005**, *38*, 176.

(20) IZA http://www.iza-structure.org/databases.

(21) (a) Férey, G.; Serre, C.; Mellot-Draznieks, C.; Millange, F.; Surblé, S.; Dutour, J.; Margiolaki, I. *Angew. Chem., Int. Ed.* **2004**, *43*, 6296. (b) Férey, G.; Mellot-Draznieks, C.; Serre, C.; Millange, F.; Dutour, J.; Surblé, S.; Margiolaki, I. *Science* **2005**, *309*, 2040. (c) Fang, Q. R.; Zhu, G. S.; Sun, J. Y.; Wei, Y.; Qiu, S. L.; Xu, R. R. *Angew. Chem., Int. Ed.* **2005**, *44*, 3845. (d) Fang, Q. R.; Zhu, G. S.; Xue, M.; Sun, J. Y.; Qiu, S. L. *Dalton Trans.* **2006**, 2399.

(22) (a) Tian, Y. Q.; Cai, C. X.; Ren, X. M.; Duan, C. Y.; Xu, Y.; Gao, S.; You, X. Z. *Chem.−Eur. J.* **2003**, *9*, 5673. (b) Cui, G. H.; Li, J. R.; Tian, J. L.; Bu, X. H.; Batten, S. R. *Cryst. Growth Des.* **2005**, *5*, 1775. (c) Park, K. S.; Ni, Z.; Côté, A. P.; Choi, J. Y.; Huang, R. D.; Uribe-Romo, F. J.; Chae, H. K.; O'Keeffe, M.; Yaghi, O. M. *Proc. Natl. Acad. Sci. U.S.A.* **2006**, *103*, 10186. (d) Hayashi, H.; Côté, A. P.; Furukawa, H.; O'Keeffe, M.; Yaghi, O. M. *Nat. Mater.* **2007**, *6*, 501.

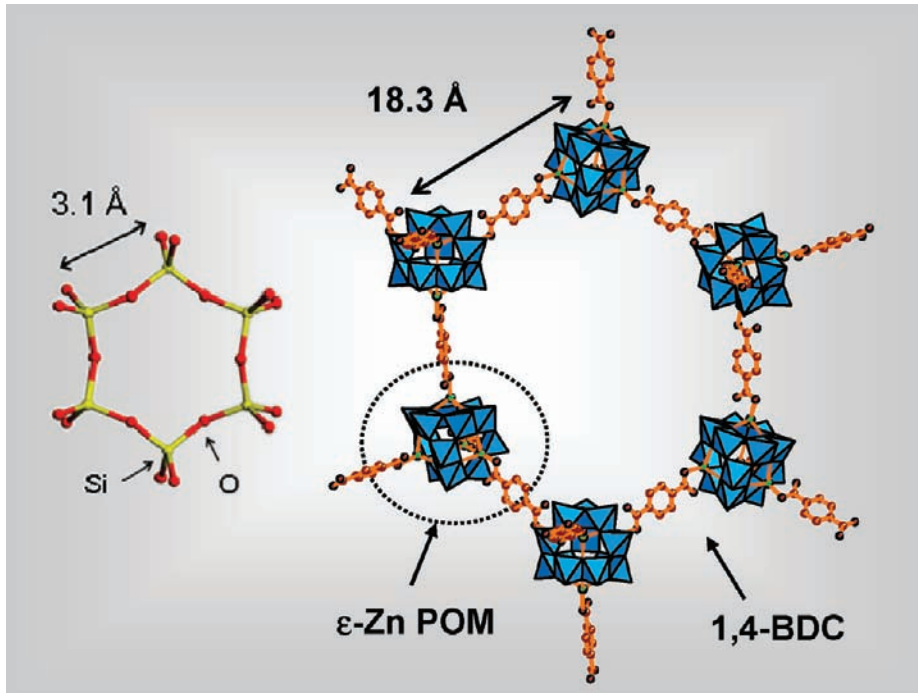

Figure 1. Schematic analogy between the structure of a silicate and that of a Z-POMOF.

for the design of a Z-POMOF are the choice of a suitable cationic POM together with that of a suitable organic linker. The cationic POM must possess an overall tetrahedral symmetry to replace the Si of the parent SiO_2 tetrahedral net, and the linker between POMs should be a rigid bifunctional anionic ligand to mimic the role of oxygen in the parent silicate structure (Figure 1). For the POM, we have turned to our recently developed family of compounds based on the ε-Keggin isomer of the reduced $\{PMo_{12}O_{40}\}$ anion.[23] We chose the Zn(II) derivative, denoted ε-Zn, instead of the La(III) derivative, as the external Zn coordination sites are likely to adopt a tetrahedral arrangement. Moreover, it has already been shown that, under hydrothermal conditions, the in situ formed ε-Zn can react with a bifunctional ligand such as 4,4′-bipyridine,[11,24] resulting in a framework comprising POM−Zn−L−Zn−POM linkages. Regarding the ligand, we chose the rigid 1,4-benzenedicarboxylate (1,4-BDC) to form the targeted POM−Zn−L−Zn−POM linkages, as 1,4-BDC is a common linker in large porous and robust MOF materials. This is a linear ligand that is unable to provide T−L−T (T = tetrahedral element) angles around 140−150° like those found in zeolites. However, our purpose here is to consider zeolites as connected tetrahedral nets and to replace the flexible T−T−T connections encountered in zeolites (typically between 75 and 145° for Si) by POM−POM−POM connections, specifically replacing Si−O−Si bridges with POM−BDC−POM links.

Model Building and Optimization. We can now consider the likely geometry and stability of a range of Z-POMOF models based on ε-Zn and 1,4-BDC, in an attempt to identify a priori which are likely to be synthetically feasible. However, due to the large number of known (and even greater number of hypothetical) tetrahedral nets,[18] we constrain our initial survey to a selection of zeotypes. Our choice was guided by noting the intriguing fact that the majority of the zeolite-like MOFs reported possess uninodal topologies, that is, have one crystallographic tetrahedral site in their asymmetric unit. We therefore took 21 known uninodal zeolites from the IZA database of zeolite structures,[20] together with a selection of dense SiO_2 structures (α-quartz, cristobalite, coesite) as the latter are known to be among the most thermodynamically favored dense minerals.

In order to construct suitable starting models of Z-POMOFs for simulations, we need to take each uninodal zeolite crystal structure and convert them to the targeted ε-Keggin and 1,4-BDC-based POMOFs. Here, we applied TOBUNPOROUS,[25] a general code written to (i) automatically replace each SiO_4 tetrahedron with an ε-Keggin ion with the appropriate orientation—here with the Zn metal centers placed along the directions defined by Si−O bonds; (ii) replace the bridging oxygen of the Si−O−Si bridge by a linking ligand—here 1,4-BDC; and finally (iii) scale the unit cell dimensions appropriately. As discussed above, our choice of networks considered was initially constrained to uninodal zeolite types. We also considered the fact that these structures ensure sampling of a range of ring sizes observed in known zeolites—from the large 12-rings found in FAU to the strained 3-rings (RWY, NPO), allowing us to explore a significant range of framework densities and structural motifs.

These initial models were subjected to lattice energy minimization in *P*1 symmetry to determine the equilibrium structures at constant pressure (i.e., including relaxation of the cell parameters) and their relative lattice energies. Since our models have a very large number of atoms (each ε-Zn and BDC ligand possess 57 and 16 atoms, respectively), energy minimization using a (molecular mechanics) forcefield is the only feasible approach for this initial stage. Our choice of forcefield is dictated by the need to consider a range of bonding types, and thus the so-called universal force field (UFF)[26] was selected, as it has suitable parameters for the systems to be considered. Bond parameters for describing Zn−O bonds were modified in order to reproduce the Zn−O distance typically observed in most solids and were fitted to the structure of ZnO, as its bonds are similar to those observed in Zn−O bearing MOFs. Since in UFF the Zn−O bond is described by the sum of four terms (eq 2 in ref 26), we varied the atomic radii to obtain the

(23) Mialane, P.; Dolbecq, A.; Lisnard, L.; Mallard, A.; Marrot, J.; Sécheresse, F. *Angew. Chem., Int. Ed.* **2002**, *41*, 2398.
(24) Lei, C.; Mao, J.-G.; Sun, Y.-Q.; Song, J.-L. *Inorg. Chem.* **2004**, *43*, 1964.
(25) Ruiz-Salvador, A. R., Gomez, A. *TOBUNPOROUS* (code available on request from the authors).
(26) Rappé, A. K.; Casewit, C. J.; Colwell, K. S.; Goddard, W. A., III; Skiff, W. M. *J. Am. Chem. Soc.* **1992**, *114*, 10024.

required bond length, resulting in a value of 1.503 Å for the Zn radius. We further constrained the simulations, given some concerns about the transferability of the potentials to such systems, to reduce the computational expense. Thus the ε-Keggin and the 1,4-BDC linker were treated as rigid bodies, while the inter-SBU (SBU = secondary building unit) interactions were ensured through Zn−O bonds free to relax between the ε-Keggin and oxygen atoms of the organic linkers; the unit cell was, however, allowed to optimize. Assigning such rigid motion groups has the advantage of preserving the complex geometry of the ε-Keggin, while allowing the ε-Keggin and the ligand to re-orient relative to one another, providing the required framework flexibility. The non-bonded interactions between pairs of atoms are represented by Lennard-Jones potentials, calculated in real space within relevant cutoffs, plus a Coulombic term, evaluated by the Ewald summation, to describe the electrostatics. The atomic charges for each Z-POMOF model were calculated by the charge-equilibrium method,[27] and the average value was then taken and fixed for all of the Z-POMOF structures, so that the same set of charges was used throughout and artifact variations of the electrostatic term among the Z-POMOFs structures thus avoided (see Supporting Information). The minimized lattice energy of each Z-POMOFs structure is normalized to the number of POMs per unit cell in the structure.

We also considered, after its synthesis, a model directly derived from the structure of Z-POMOF1 (described below). Thus, the experimental crystal structure of triply interpenetrated Z-POMOF1 was converted into its silica polymorph, and the latter was then converted back into its POMOF analogue to ensure that the lattice energy of the experimental interpenetrated topology could be determined in exactly the same fashion as the other simulated Z-POMOFs. We also compared the stability of the interpenetrated network with that of each single network to establish the influence of interpenetration on structural stability. The model of the interpenetrated cristobalite-like network is referred to as Z-POMOF1, while the single-net version is referred to as Z-POMOF1 (single net).

Synthesis and Characterization. Hydrothermal synthesis of Z-POMOF1 was carried out in PTFE lined stainless steel containers under autogenous pressure. The 23 mL vessel was filled to approximately 40% volume capacity. Commercially available reagents were used as received, without further purification. All reactants were stirred briefly before heating. Z-POMOF1 was prepared from a mixture of $(NH_4)_6Mo_7O_{24}\cdot 4H_2O$ (0.618 g, 3.50 mmol), 99.99% molybdenum powder (0.060 g, 0.62 mmol), H_3PO_3 (0.020 g, 0.25 mmol), $ZnCl_2$ (0.136 g, 1.00 mmol), 1,4-benzenedicarboxylic acid (0.166 g, 1.00 mmol), 40 wt % tetrabutylammonium hydroxide solution in water (160 μL, 0.24 mmol), and H_2O (9 mL). The pH was adjusted to 5 (pH_i) with 2 M HCl (pH_f = 4.7). The mixture was heated to 180 °C in 1 h, and the temperature was maintained for 40 h and then cooled to room temperature over a period of 80 h. The product was isolated by filtration and separated from an amorphous brown powder and white crystals by decantation and washed with ethanol. Dark red, almost black, hexagonal crystals suitable for X-ray diffraction study were collected (0.113 g, 14% based on H_3PO_3). NMR and FTIR spectra and elemental analyses are given in the Supporting Information.

X-ray diffraction was carried out with a Siemens SMART three-circle diffractometer equipped with a CCD bidimensional detector using the monochromatized wavelength λ (Mo Kα) = 0.71073 Å. Absorption correction was based on multiple and symmetry-equivalent reflections in the data set using the SADABS program[28] based on the method of Blessing.[29] The structure was solved by direct methods and refined by full-matrix least-squares using the SHELX-TL package.[30] The disordered C atoms of the tetrabutylammonium counterions were refined isotropically. Crystallographic data are given in Table 1, and a CIF file is available in Supporting Information. Temperature-dependent X-ray diffraction was performed on a Siemens D-5000 diffractometer in the $\theta-\theta$ mode under air. Each pattern was recorded in the range 7−35° (2θ) with a 2 s per step scan, which gave an approximate scan time of 1 h for each pattern at any given temperature. The heating rate between two temperatures was 5 °C min^{-1}. Thermogravimetry was carried out under N_2/O_2 (1:1) flow (60 mL min^{-1}) with a Perkin-Elmer electrobalance TGA-7 at a heating rate 5 °C min^{-1} up to 800 °C.

Table 1. Crystallographic Data for Z-POMOF1

empirical formula	$C_{64}H_{124}Mo_{12}N_3O_{50}P$
formula weight, *g*	3179.5
crystal system	monoclinic
space group	*C*2/*c*
a/Å	15.0956(11)
b/Å	27.0921(19)
c/Å	25.7271(18)
β/deg	106.834(2)
V/Å^3	10070.8(12)
Z	8
ρ_{calcd}/g cm^{-3}	2.096
μ/mm^{-1}	2.476
data/parameters	14675/490
R_{int}	0.0580
GOF	1.090
R (>2σ(*I*))	$R_1{}^a = 0.0624$
	$wR_2{}^b = 0.1303$

^{a} $R_1 = \sum|F_o| - |F_c|/\sum|F_c|$. ^{b} $wR_2 = \sqrt{\sum w(F_o^2 - F_c^2)^2/\sum w(F_o^2)^2}$.

Electrochemistry. Cyclic voltametry (CV) analysis was performed using a number of different Z-POMOF1-modified electrode techniques. Details on the experimental conditions used for this study are given in the Supporting Information.

Results and Discussions

Computational Simulations. We will describe the results in chronological order and thus begin by discussing the results of the computational simulations. The relaxed Z-POMOF candidates were analyzed in terms of their geometrical features, and relative energies and are presented in Figure 2. It is noteworthy that no Z-POMOF model resulted in an unstable structure, but all models exhibited moderate reorientation of the organic ligand and similar Zn−O bonds distances of between 2.04 and 2.08 Å. We focus here on the relationship between the topology and porosity (i.e. density) and the total lattice energy (Figure 3) that we use to guide our synthetic work.

In a similar fashion to that found for silicates,[31] the compact structures of α-quartz-, cristobalite-, and coesite-like Z-POMOFs are among the most stable structures. However, in contrast to the silica polymorphs, the α-quartz topology is not the most stable structure; rather it is the cristobalite-like (or diamond) Z-POMOF which is favored. Indeed, it is noteworthy that, within MOFs, cristobalite-like (or diamond-like) hybrid frameworks are the most prevalent dense structures: among tetrahedral MOFs, 70% have this topological net.[19] Moreover, we again note that it was this cristobalite topology which was formed first in the ZIF family as Zn{azabenzimidazole}$_2$,[22d] and similarly as Cd(Imazethapyr)$_2$ (Imazethapyr = 2-(4,5-dihydro-4-methyl-4-(1-methylethyl)-5-oxo-1*H*-imidazol-2-yl)-5-ethyl-3-pyridinecarboxylate)[32] and Co(imidazole)$_2$.[22a] However, these MOF materials are often obtained as interpenetrated networks.

(27) Rappé, A. K.; Goddard, W. A., III. *J. Phys. Chem.* **1991**, *95*, 3358.
(28) Sheldrick, G. M. *SADABS*, program for scaling and correction of area detector data; University of Göttingen: Germany, 1997.
(29) Blessing, R. *Acta Crystallogr.* **1995**, *A51*, 33.
(30) Sheldrick, G. M. *SHELX-TL*, version 5.03; Software Package for the Crystal Structure Determination; Siemens Analytical X-ray Instrument Division: Madison, WI, 1994.
(31) Henson, N.; Cheetham, A. K.; Gale, J. D. *Chem. Mater.* **1994**, *6*, 1647.
(32) Fu, D.-W.; Zhang, W.; Xiong, R.-G. *Dalton Trans.* **2008**, 3946.

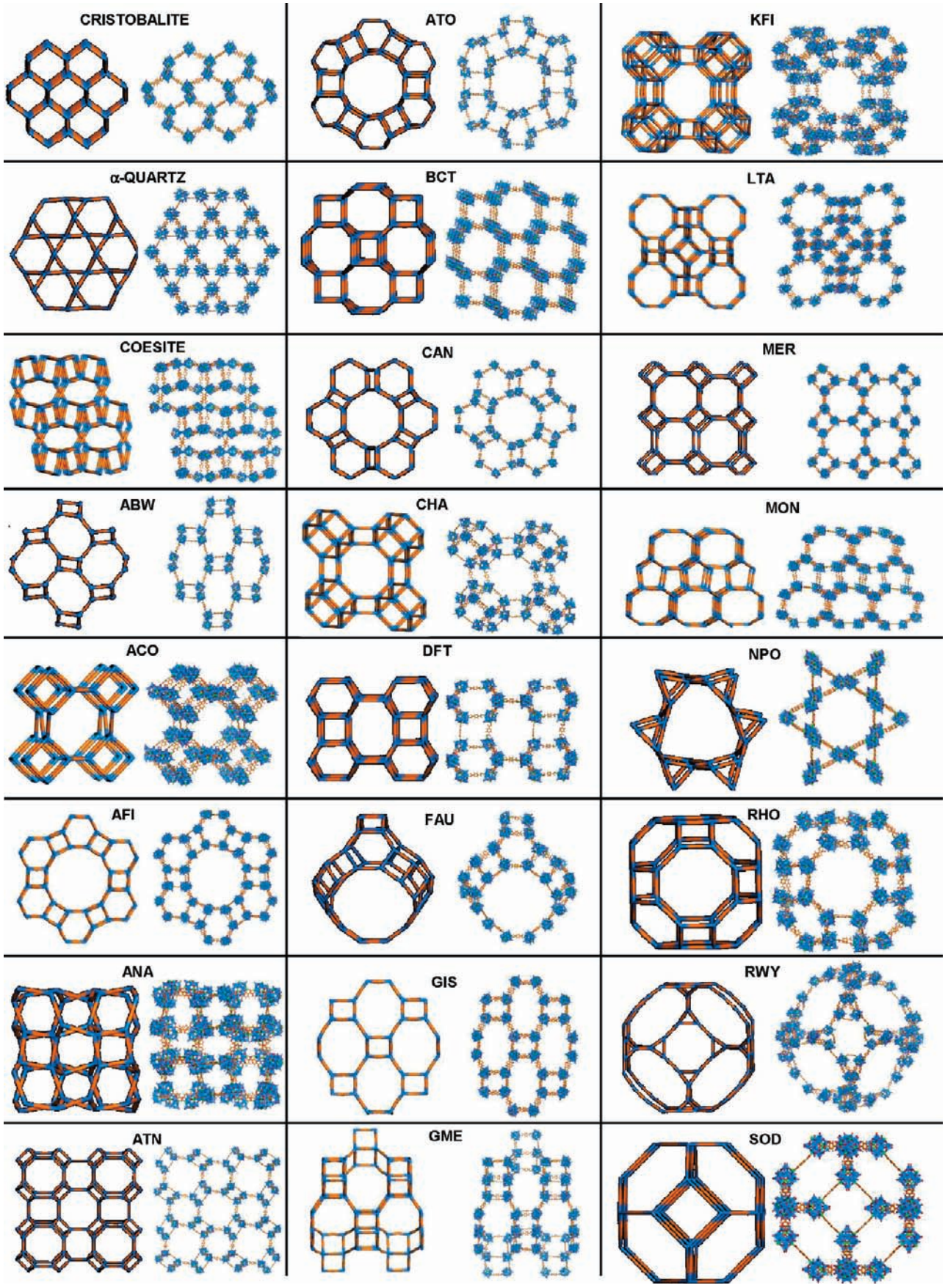

Figure 2. Simulated crystal structures of Z-POMOFs. In each box, the zeotype or mineral net is shown as a stick diagram (left), while the corresponding Z-POMOF is shown with a polyhedral representation of the ε-Keggin ion (blue); the 1,4-BCD is shown in orange.

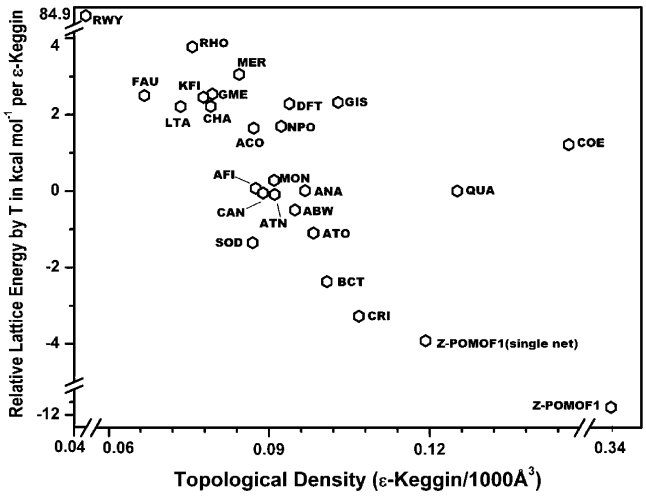

Figure 3. Variation of lattice energies of Z-POMOFs with density expressed as the number of ε-Keggin per unit cell.

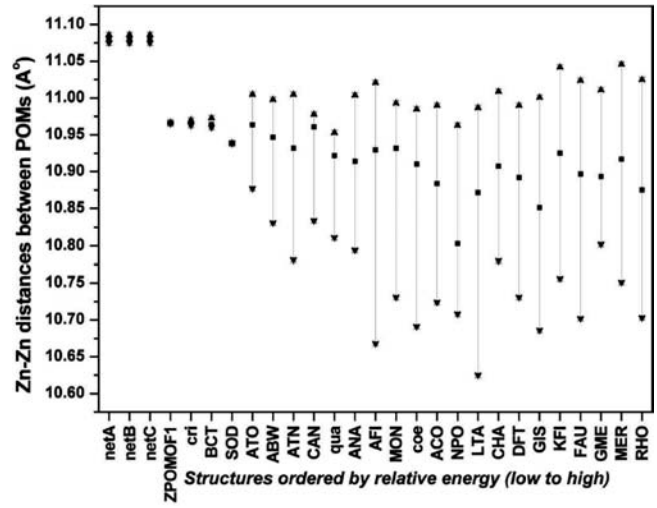

Figure 4. Plot of Zn−Zn distances as measured between POMs (internal Zn−Zn to the ε-Keggin are ignored) throughout all Z-POMOFs. The structures are ranked from the most stable one to the least stable. The squares represent average Zn−Zn distances in each structure. Nets A, B, and C refer to each of the three nets of the interpenetrated Z-POMOF1 structure.

Turning to the zeolitic Z-POMOFs, we find a rather restricted range (∼7 kcal mol^{-1}) of computed lattice energies from the least stable RHO and the most stable BCT (if we neglect what appears to be the atypical case of RWY). Care must be taken, however, not to place too great an emphasis on the absolute quantitative results as they are primarily a consequence of the choice of forcefield. Nevertheless, we believe that it is probable that the qualitative trends observed will be maintained regardless of forcefield choice. It is apparent that there is an approximately linear trend of lattice energies with density, reminiscent of the variation in relative lattice energies of siliceous zeolites,[31] where a direct dependence of lattice energy on density is found. Similarly, three-membered rings are, as in silicates, seemingly unfavored, as revealed by RWY being particularly unstable. However, the trend is less apparent than in the silicates, perhaps suggesting a richer variety of structures may be accessible.

There have been a number of attempts to elucidate what dictates the fundamental stability of a tetrahedral net, focused mainly on inorganic zeolitic materials. When silica polymorphs are considered, there is considerable flexibility in forming rings since the Si−O−Si angle can vary quite significantly: indeed it is only three-membered rings which appear particularly strained, which of course correlates well with the absence of pure silica zeolites with such rings. Here, the presence of a rigid organic linker, together with the need to maximize orbital overlap between the metal centers of the POM and oxygen atoms on the linker, reduces the range of acceptable POM−linker−POM connections. Indeed, we may deduce that the topologies most likely to form are those that allow the formation of rings where the *com*POM−BDC−POM*com* angle is linear (*com* indicates that the center of mass of the POM is taken under consideration), which will result in the most symmetric rings (and hence topologies) being favored over those with distorted or puckered rings. We therefore consider as a measure of ring distortion the inter-POM Zn−Zn distances in the optimized structures (Figure 4). It is quite clear that the most stable structures are those with the narrowest distribution of such distances. Moreover, it is now perhaps apparent why the cristobalite net is favored here over the α-quartz structure and more generally in MOFs. Encouragingly, however, a number of the energetically more stable Z-POMOF structures also exhibit a small amount of distortion, such as BCT and SOD. We can extend such a geometric analysis, and we find that the group of lowest energy Z-POMOF structures all contain four-membered rings which are perfectly flat, followed by a grouping which shows some distortion of the 4-ring but which shares a corner with another 4-ring, and then a grouping where again the 4-rings are flat but which edge-share with another 4-ring at an angle less than the "optimal" tetrahedral angle. Such observations lead us to suggest that a simple geometric analysis of the parent tetrahedral nets may be sufficient as an initial screen of further known and hypothetical nets, in order to identify possible synthesis targets.

It is clear that of all the structures considered the most dense structures are those which are most thermodynamically stable and hence the most likely to form through a hydrothermal synthesis approach. However, it is also encouraging that a number of zeotypic structures, such as BCT, SOD, and ATO, are close in energy, for reasons discussed above, to these more dense materials, suggesting that these may also be suitable targets for synthesis. Indeed, in light of our successful synthesis of cristobalite-like material here (as discussed below), BCT and SOD appear likely synthesis targets.

Synthesis and Characterization. Encouraged by our simulation results, we devised an attempt at a synthesis of a Z-POMOF. As it had not been possible to date to isolate a soluble salt of the ε-Zn POM precursor, the formation of the species was induced in situ under hydrothermal conditions. Our synthesis of Z-POMOF1 was thus performed by the reaction of $(NH_4)_6Mo_7O_{24}$, Mo as reducing agent, H_3PO_3, $ZnCl_2$, 1,4-benzenedicarboxylic acid (1,4-H_2BDC), and TBAOH (TBA = tetrabutylammonium) in water at 180 °C. The value of the initial pH (around 5.0) is critical, as is the presence of the TBA^+ cations, which act not simply as space-filling agents but also as counterions and potentially as structure-directing agents. Indeed, attempts to replace the TBA^+ with smaller cations, specifically NH_4^+, tetramethylammonium, and tetraethylammonium, failed, suggesting some degree of structure-directing action. For example, dark blue crystals of the four-electron-reduced $\{PMo_{12}O_{40}\}$ species were formed in the presence of tetraethylammonium (see Supporting Information).

The infrared spectrum of Z-POMOF1 clearly shows the presence of C−O vibrational bands around 1573 and 1362 cm^{-1}.

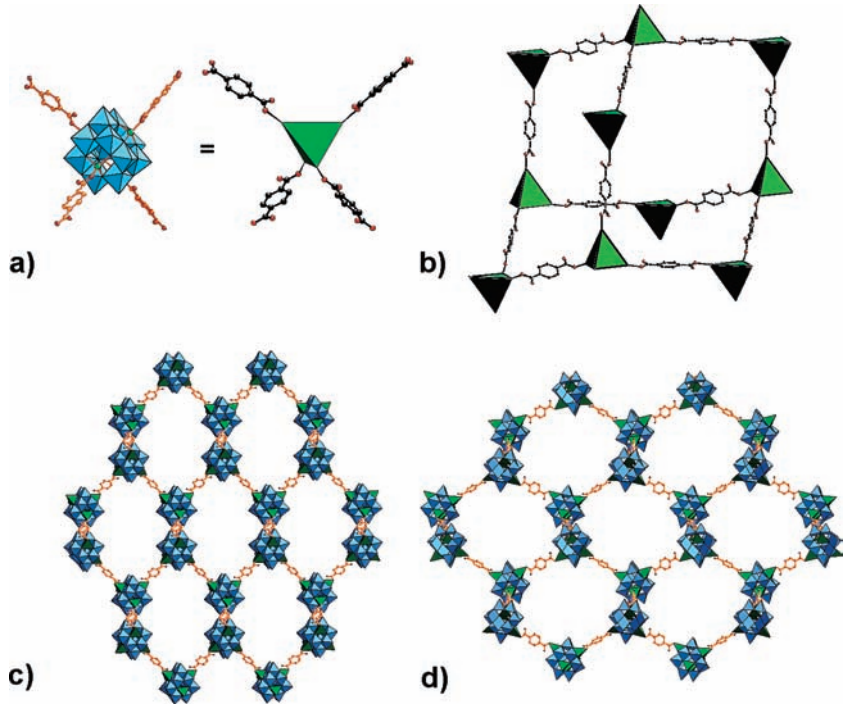

Figure 5. (a) Representation of the coordination mode of the ε-Zn POM in Z-POMOF1 and of its schematized structure. (b) Adamantane-like unit of Z-POMOF1. View of a single network of (c) the experimental Z-POMOF1 and (d) the cristobalite-like model.

The large difference between the antisymmetric and symmetric C−O stretching frequencies ($\Delta\nu = 211$ cm^{-1}) indicates monodentate coordination of each carboxylate group to the POM. The bands at 1482, 1464, and 1383 cm^{-1} can be attributed to the TBA$^+$ cations, and the bands at 938, 890, 815, 786, 745, and 709 cm^{-1} are assigned to Mo−O vibrations. Z-POMOF1 is slightly soluble in DMSO, the dissolution being due to the dissociation of the single Zn−O(C) bond between the ε-Zn POM and the BDC ligand. ^{31}P and ^{1}H NMR spectra of a saturated solution of Z-POMOF1 have been recorded (Figure S1 in Supporting Information). The presence of a single peak at −2.59 ppm is observed by ^{31}P NMR spectroscopy. This spectrum does not evolve over a period of 1 week, indicating that the ε-Zn POM is stable in solution, in contrast to the observation of equilibrium between species with four La ions and species with only three capping rare earth cations in ε-La POMs.[23] Signals attributed to TBA$^+$ cations and the BDC ligand can be identified on the ^{1}H NMR spectrum, and the integration confirms a TBA/BDC ratio of 3/2 in the product.

Crystal Structure of Z-POMOF1. The crystal structure of a single net of Z-POMOF1 (Figures 5a−c) is compared to that of the predicted cristobalite-like Z-POMOF (Figure 5d). The inorganic building unit of the ε-PMo_{12} isomer capped by four Zn(II) ions (Figure 5a) maintains an overall tetrahedral symmetry in the Z-POMOF1 structure. As in the structures of ε-La and ε-Zn derivatives,[11,12,23,24] the Keggin ion is an eight-electron-reduced POM, containing 8 Mo(V) and 4 Mo(VI) ions, as confirmed by the short Mo(V)−Mo(V) bonds (∼2.6 Å) as well as bond valence sum calculations on the Mo centers (Table S1 in Supporting Information). The four Zn ions are grafted to the ε-$PMo_{12}O_{40}$ POM via three Zn−O(Mo) bonds with bridging oxygen atoms and complete their tetrahedral coordination sphere with a Zn−O(C) bond to a BDC ligand: monodentate Zn−BDC link is again found, in agreement with the FTIR data. The connection of the POMs results from the bifunctionality of the organic ligand, generating a 3-D framework reminiscent of the structure of cristobalite-like (diamond) network. The adamantane-like unit of Z-POMOF1 is shown in Figure 5b, and a view of one coordination network along the *a*-axis is presented in Figure 5c and along the *b*-axis in Figure 6a. Z-POMOF1 actually comprises three independent interpenetrating cristobalite-like networks as shown by Figures 6b,c. Channels are present along the crystallographic *a*-axis (Figure S2 in Supporting Information). The channels are filled by TBA$^+$ countercations, with three TBA$^+$ cations per POM unit being clearly identified in the Fourier difference map and their presence being confirmed both by elemental analysis and by ^{1}H NMR (see above). The charge on ε-Keggin units depends on the number of the protonated oxo bridging ligands and has been shown to vary from 0 to 5 in eight-electron-reduced ε-PMo_{12} derivatives.[11,12,23,24] In Z-POMOF1, the presence of four protons, which are located on four bridging oxygen atoms, as indicated by BVS calculations (Table S1 in Supporting Information), is required for charge neutrality reasons. The detailed formula of Z-POMOF1 is thus $[TBA]_3[PMo^{V}_8Mo^{VI}_4O_{36}(OH)_4Zn_4(BDC)_2]\cdot 2H_2O$ and the formula of the inorganic building unit $\{PMo^{V}_8Mo^{VI}_4O_{36}(OH)_4Zn_4\}^+$.

A comparison of the solvent-accessible voids of Z-POMOF1, calculated using PLATON,[33] with and without the localized TBA$^+$ cations is striking. The solvent-accessible volume reduces from 60% of the total volume of the unit cell (6042 Å^3, which represents around 150 water molecules assuming a volume of 40 Å^3 for a hydrogen-bonded water molecule) to 5.6% when the TBA$^+$ cations are present. The accessible volume would be higher still if there was no interpenetration of the cristobalite-like networks. It has been well-documented that interpenetration is one consequence of large voids.[34] Three-fold interpenetration is thus common in cristobalite-like (or diamond-like) struc-

(33) Spek, A. L. *J. Appl. Crystallogr.* **2003**, *36*, 7.
(34) (a) Batten, S. R.; Robson, R. *Angew. Chem., Int. Ed.* **1998**, *37*, 1460. (b) Batten, S. R. *CrystEngComm* **2001**, 67.

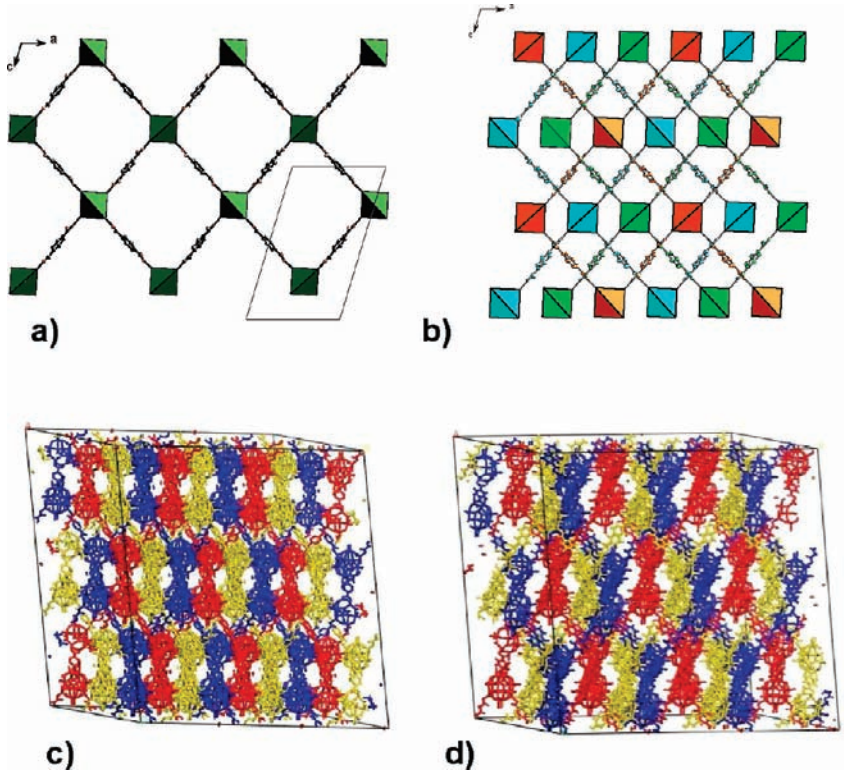

Figure 6. Schematic representation (a) of one network along the *b*- axis in Z-POMOF1 and (b) of the three interpenetrated networks, each one having a different color. Complete view of the three interpenetrated networks (c) in the experimental structure and (d) in the modeled structure.

tures.[35] TBA^+ ions play the role of space-filling agents but also of charge-compensating cations. If TBA^+ were not present, three additional protons (or other extra-framework cations) would be necessary to compensate the charge. However, structures of eight-electron-reduced ε-PMo_{12} derivatives with seven protonated oxo bridges have not been observed to date, which may further account for the presence of the alkyammonium counterions.

In order to demonstrate and quantify the role of interpenetration on the stability of Z-POMOF1, we consider models consisting of both the whole interpenetrated structure and a single net, with the same POMOF composition as those previously modeled. Both the three-fold interpenetrated modeled structure (Figure 6d) and the single net (Figure 5d) are in reasonably good agreement with their experimental counterparts in Z-POMOF1 (Figures 6c and 5c, respectively), suggesting the single net is robust. However, note that optimization of these reconstructed models does differ from the synthesized material by 5.6, 8.2, and −2.0% along the *a*, *b*, and *c* directions, respectively. The absence of water and TBA^+ cations in these models probably accounts for the majority of these differences, as observed in other modeling studies of framework solids.[36] Considering now the relative stability of the single and interpenetrated networks indicated in Figure 3, it is remarkable that the energy of the interpenetrated Z-POMOF1 is considerably lower (∼8 kcal/mol) than our model cristobalite-like network and Z-POMOF1 (single net). The simulations thereby provide a direct estimation of the net−net interactions (∼7 kcal/mol), indicating the added stabilization achieved through the formation of the more dense and interpenetrated structure.

(35) Blatov, V. A.; Carlucci, L.; Ciani, L.; Proserpio, D. M. *CrystEngComm.* **2004**, *6*, 377.
(36) Ruiz-Salvador, A. R.; Almora-Barrios, N.; Gómez, A.; Lewis, D. W. *Phys. Chem. Chem. Phys.* **2007**, *9*, 521.

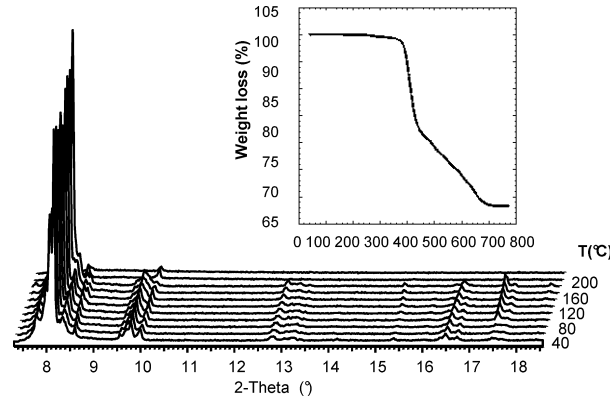

Figure 7. X-ray thermodiffractogram of Z-POMOF1 under air. Inset: TGA under air.

The crystalline structure of Z-POMOF1 is maintained up to 180 °C, as revealed by the variable temperature X-ray diffraction experiments (Figure 7), which correlates to the TGA data. In the latter, no weight loss is observed between 25 and 180 °C (Figure 7, inset). Between 180 and 380 °C, a small weight loss (around 0.7%) is detectable and could be attributed to the dehydration of the material. A two-step weight loss is then observed between 380 and 700 °C, with a total weight loss of 32% (calcd 31%), corresponding to the breakdown of the framework and then of its components, leading to the formation of oxides (MoO_3, ZnO, and P_2O_5). This thermal behavior is strikingly different from that of ε-La POM-based MOFs, which collapse above 50 °C,[11] confirming that ε-Zn POMs provide a viable route to further, stable 3-D porous frameworks.

Electrocatalytic Behavior of Z-POMOF1 toward Bromate. Prior to electrocatalytic studies, a detailed solid-state electrochemical examination of Z-POMOF1 was performed and is

described in the Supporting Information. The solid-state electrochemistry was carried out by entrapping the POMs in a carbon paste (CPE)[37] or in polyvinyl alcohol (PVA). Briefly, cyclic voltammetry experiments have shown that the electrochemical activity of the reduced species of ε-PMo_{12} building units is maintained but with a clear influence of their incorporation in Z-POMOF1. ε-Zn in Z-POMOF1 exhibits three waves featuring three consecutive bielectronic processes (Figure S3 in Supporting Information). The striking observation is the splitting of the third wave of ε-Zn into two waves smaller than the corresponding wave of ε-La. The splitting of this wave should be associated with the acid−base properties of the reduced species of ε-Zn. Thus, an electrochemical−chemical−electrochemical (ECE)- or electrochemical−electrochemical−chemical (EEC)-type process inducing waves merging seems to be more favorable with ε-La in the pH 2 medium.

Thus the Z-POMOF1-modified electrodes are good candidates for applications in electroanalysis and electrocatalysis. To illustrate their potential, we consider the reduction of bromate, already the subject of study using POMs.[38] The monitoring or removal of this species is of interest as it is present in drinking-water samples as a byproduct of ozone disinfection and is often used as food additive. However, bromate is suspected to act as a human carcinogen.[39] We found that both Z-POMOF1-CPE and PVA-modified electrodes (Z-POMOF1-PVAE) are active for electrocatalytic reduction of bromate. In the following, however, we restrict our discussion to PVAEs. While the fabrication of Z-POMOF1-CPE is straightforward, PVAEs have added advantages, including the possibility of elaboration of large surface area electrodes with various materials.

Figure 8 illustrates the ability of Z-POMOF-PVAE to electrocatalyze the reduction of bromate. In the explored potential domain, glassy carbon modified only with PVA does not show any electrocatalytic activity for bromate reduction. The onset of the catalytic process is at about 0.130 V relative to a SCE and is triggered by the second wave of ε-Zn (Figure 8a). Upon increasing bromate concentration, the cathodic current of the second reduction wave rises and the corresponding anodic current gradually decreases. This reaction has been described with other POMs in the literature as a six-electron process, yielding bromide.[40] The onset potential observed here compares favorably with reported values. As expected, the onset potential shifts toward the positive direction when the pH of the electrolyte decreases. A linear correlation is found between bromate concentration and current (Figure 8b), in the range 0.2 to 40 mM of bromate, thus opening the way for detection, quantification, and transformation of this chemical by Z-

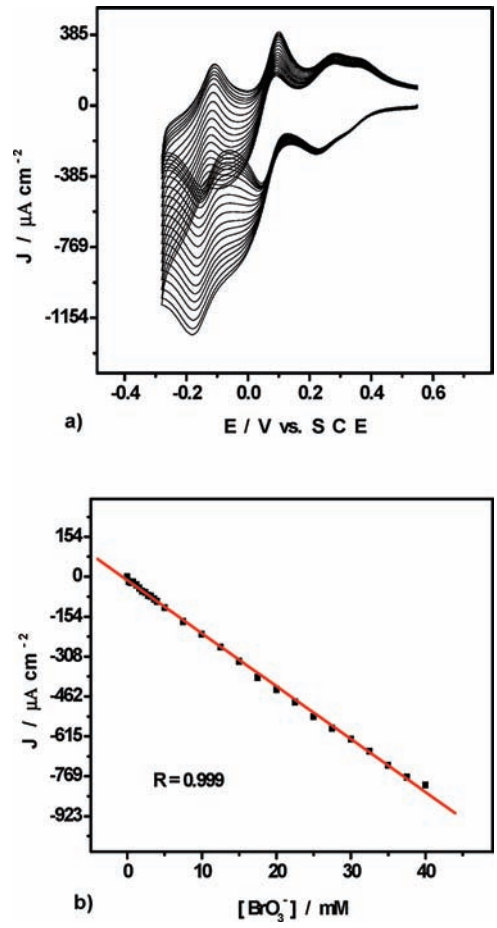

Figure 8. (a) CVs of Z-POMOF1-PVAE in a pH 2 medium (1 M LiCl/HCl) in the absence and upon addition of increasing concentrations of bromate. (b) Variation of the peak current intensity for bromate electrocatalytic reduction as a function of its concentration (third wave). The scan rate was 50 mV s^{-1}. The reference electrode was a saturated calomel electrode (SCE).

POMOFs. A sharp decrease of activity was observed for pH values lower than 1.5, with the POM $H_3PMo_{12}O_{40}$ immobilized on 3-aminopropyltrimethoxysilane electrode.[41] In contrast, it is worth noting that Z-POMOF1-PVAE exhibits high activity even at pH 2. With such promising results, immobilization of Z-POMOFs on various substrates including carbon nanotubes is envisioned. Other challenging electrocatalytic processes such as reduction of chlorate, iodate, hydrogen peroxide, and NO_x will be explored. In addition, it is expected that new Z-POMOFs with appropriate compositions will expand application domains.

Conclusion

This study has shown that a new extension of the MOF family of solids is possible, by demonstrating the synthesis of a novel three-dimensional zeolitic polyoxometalate-based metal−organic framework (Z-POMOF). Z-POMOF1 could, of course, have been synthesized without preliminary simulations. However, our combined simulation/experiment approach more generally suggests that a rich family of Z-POMOFs is possible, given the number of modeled structures that have a stability similar to that of the material synthesized, Z-POMOF1. Moreover, we have identified certain geometric features which may be useful to prescreen topologies for potential synthesis.

(37) (a) Adams, R. N. *Anal. Chem.* **1958**, *30*, 1576. (b) Marcoux, L. S.; Prater, K. B.; Prater, B. G.; Adams, R. N. *Anal. Chem.* **1965**, *37*, 1446. (c) Rice, M. E.; Galus, Z.; Adams, R. N. *J. Electroanal. Chem. Interfacial Electrochem.* **1983**, *143*, 89. (d) Wang, J; Naser, N.; Angnes, L.; Wu, H.; Chen, L. *Anal. Chem.* **1992**, *64*, 1285. (e) Lubert, K.-H.; Guttmann, M.; Beyer, L. *J. Electroanal. Chem.* **1999**, *642*, 174. (f) Kim, G.-Y.; Cuong, N. M.; Cho, S.-H.; Shim, J.; Woo, J.-J.; Moon, S.-H. *Talanta* **2007**, *7*, 129. (g) Wang, X.-L.; Wang, E.-B.; Lan, Y.; Hu, C.-W. *Electroanalysis* **2002**, *14*, 1116. (h) Keita, B.; de Oliveira, P.; Nadjo, L.; Kortz, U. *Chem.−Eur. J.* **2007**, *13*, 5480.

(38) (a) Keita, B.; Nadjo, L. Electrochemistry of Isopoly and Heteropoly Oxometalates. In *Encyclopedia of Electrochemistry*; Bard, A. J., Stratmann, M., Eds.; Wiley-VCH: Weinheim, Germany, 2006; Vol. 7, pp 607−700. (b) Keita, B.; Nadjo, L. *J. Mol. Catal. A* **2007**, *262*, 190.

(39) (a) Do-Quang, Z., Baudin, I. IWA Publishing: London, UK, 2008. (b) Moore, M. M.; Chen, T. *Toxicology* **2006**, *221*, 190–196. (c) Bonacquisti, T. P. *Toxicology* **2006**, *221*, 145–148.

(40) Hill, C. L. *Chem. Rev.* **1998**, *98*, 1–389 (guest editor).

(41) Rahman, Md.A.; Won, M.-S.; Wei, P.-H.; Shim, Y.-B. *Electroanalysis* **2006**, *18*, 993–1000.

Our material, Z-POMOF1, in addition to having a cristobalite-like three-fold interpenetrated structure, also contains tetrabutylammonium cations in charge-compensating, space-filling, and, we believe, to an extent, a structure-directing role. Further experiments are underway in order to determine if the structure can be rendered porous, specifically by (i) replacement of the Zn with trivalent cations, increasing the positive charge of the ε-Zn core and reducing the overall charge on the framework; (ii) synthesis with less bulky ammonium counterions or protonated amines; and (iii) replacing BDC with neutral and bulkier organoamine ligands such as pyrazine or imidazole to lower the overall negative charge of the framework, reducing the need for counterions.

The work here has shown the feasibility of the synthesis of Z-POMOFs by comparison with the stability of the parent structures analogues. From our work, we would suggest that, here, templating strategies may prove fruitful, either, as here, using charge compensating cations or through substitution on the ligand, and may provide routes to the less stable but more open topologies.

Finally, electrodes based on Z-POMOF1 exhibit remarkable electroactivity in the reduction of bromate, with the incorporation of the POM within a framework, leading to an enhanced performance compared to the free POM.

Acknowledgment. This work was supported by the EPSRC (Advanced Research Fellowship awarded to C.M.-D.) and the FP-6-European funding STREP "SURMOF" (NMP4-CT-2006-032109) and European Union-sponsored Alfa NANOGASTOR Network (II-0493-FA-FI). Partial support from University of Havana and the Cuban National Program on Basic Sciences−CITMA (L.M.R.-A. and A.R.R.-S.) is also acknowledged.

Supporting Information Available: Details on calculations, synthesis, and electrochemistry measurements. This material is available free of charge via the Internet at http://pubs.acs.org. Simulated Z-POMOF crystal structures are available on request.

JA905009E